Structural thermodynamics of lamellar cationic lipid-DNA complex: DNA compressibility modulus

O. González-Amezcua and M. Hernández-Contreras[a)]
Departamento de Física, Centro de Investigación y Estudios Avanzados del Instituto Politécnico Nacional, A.P. 14-740, México Distrito Federal, Zacatenco CP 07360, Mexico

(Received 14 July 2005; accepted 14 October 2005; published online 14 December 2005)

We have studied theoretically the compressibility modulus B of DNA and complexation adsorption isotherms of DNA and lipids, as a function of DNA spacing d_{DNA} and NaCl electrolyte concentration, respectively, in isoelectric states of lamellar DNA/cationic lipid (CL) self-assemblies. The electrostatic free energy derived from the Poisson-Boltzmann theory predicts partial agreement with measured B values for interhelical separations $d_{\mathrm{DNA}} > 33$ Å when use is made of a fit of hydration repulsion from bulk DNA hexagonal phases in solution. For lower interchain separations the prediction worsens due to the hydration interaction that overcomes the electrostatic contribution. An exact match of the system's counterion electrochemical potentials and the coions of salt in aqueous phase leads to the electrostatic part of the free energy that renders isotherms of d_{DNA} versus ionic strength in qualitative consistency with general trends of available experimental data of CL-DNA complexes. © *2005 American Institute of Physics*. [DOI: 10.1063/1.2137697]

I. INTRODUCTION

Cationic liposomes serve as useful vehicles to transport extracellular DNA into cell cytoplasm.[1–4] In a comprehensive series of experiments, Salditt and co-workers[5–8] have determined with synchrotron x-ray scattering that DNA chains form two-dimensional (2D) lattice arrangements in the carrier liposome interior. Such self-assembled systems are being studied with the aim of using them in gene therapy.[3] However, recent *in vitro* experiments show a low rate of DNA transfection through cell and nuclear membranes.[9] Therefore, one expects that a precise knowledge of the system's microstructure will help to enhance the efficiency of the DNA delivery process.[1,6]

In their experiments Salditt *et al.*[5] measured the DNA compressibility modulus $B(d_{\mathrm{DNA}})$ as a function of interhelical spacing d_{DNA} in isoelectric systems, that is, stoichiometrically charge neutral cationic lipid (CL)-DNA complexes, where there is the same amount of cationic lipid of the liposomes and anionic DNA charges, without added salt in solution. Since cationic liposomes are made of neutral and positively charged lipids, one such system is obtained by keeping its total lipid composition constant, while the molecular weight ratio of the DNA to the cationic lipid species is kept fixed at a constant value of 2.2 to ensure an overall charge neutrality of the system. At thermal equilibrium this isoelectric complex shows an average DNA-DNA separation d_{DNA}. The compressibility modulus relates to the force per unit length of the DNA in such 2D crystalline condensed state. Salditt *et al.* demonstrated that several forces are implicated in the stability of DNA condensation. These include hydration and electrostatic forces, which are repulsive, and the attractive, but negligibly weak van der Waals force. Until now, no theoretical explanation is available on the specific way these intermolecular forces drive the cationic lipid-DNA complex stability. Salditt *et al.* discussed several possible mechanisms for the observed DNA effective repulsive force, and considered different microscopic model interactions: In order to be consistent with their observation of the line-shape analysis of scattered light, Helfrich's steric type of interaction of 2D ordered DNA strands was ruled out since it does not correspond to the lateral strand fluctuations. Also, pure hard-core chain-chain interactions cannot explain the data for $B(d_{\mathrm{DNA}})$. They found that ordering is not just an effect of close packing. On the other hand, the three-dimensional (3D) hydration interaction between DNA pairs that was found in bulk solutions to produce repulsion among DNA strands[17] cannot alone account for the experimentally measured $B(d_{\mathrm{DNA}})$.[5] Indeed Salditt *et al.* observed that long-ranged electrostatic interactions of exponential form, as found in hexagonal concentrated DNA phases, do not conform to their data of $B(d_{\mathrm{DNA}})$. For this type of interaction to be consistent with B, a fitting in the electrolyte concentration up to 14.4 mM is required. However, this concentration of counterions is much larger than the estimated of 1 mM in the interior of actual isoelectric systems.[5] Therefore, a complete comparison between the theory and the available experimental measurements of the compressibility modulus B and its dependence on the interchain distance d_{DNA} remains yet to be performed.

From the theoretical viewpoint, Bruinsma and Mashl[10] developed, at the level of mean-field Poisson-Boltzmann (PB), the first theory which leads to the long-range electrostatic contribution to B. A comparison of their PB analytical solution with the experimental data of Salditt *et al.* showed a large predicted value of B at small d_{DNA} that, however, decays faster than the data. In their model of a CL-DNA complex, Bruinsma and Mashl used an electroneutral system made of two flat positively charged membranes, each one

[a)]Electronic mail: marther@fis.cinvestav.mx

having a very low surface density of cationic lipids with an intervening embedded lattice of negatively charged rods. Therefore, the rods are separated by large distances. In this model system the finite size of the lipid is neglected and all counterions are released from the system's interior.

The observed two-dimensional DNA ordering has been successfully analyzed with the help of the theory developed by Harries *et al.*[11] This theory has been used previously to predict the complexation isotherms of the DNA interchain separation as a function of charge on the lipid membranes and fixed the overall molecular weight ratio of the lipid to DNA charges.[11,12] It was found to reproduce the general trends of the experimentally measured isotherms.[12] Based on this theory, all possible lipid-DNA composite phases were determined,[13] and the interplay of spatial corrugations and charge lipid modulations in these complexes was demonstrated.[14]

In this paper we used the theoretical approach of Harries *et al.* to obtain numerical solutions of the full nonlinear PB equation and we made a fit of a parametrized form of a hydration repulsion, including the van der Waals interaction and negligible ion size at $c^*=2$ mM electrolyte concentration. We found good agreement with the measured data of $B(d_{\mathrm{DNA}})$ to a fit of hydration repulsion at $d_{\mathrm{DNA}}>33$ Å where the electrostatic effective interaction dominates. The effective electrostatic force contains the main contribution due to the large ionic entropy force arising from the extreme counterion release upon lipid-DNA self-assembly.

However, for low values of d_{DNA} the prediction worsens due to the high strength of the hydration repulsion that overwhelms the electrostatic contribution.

For another set of experimental measurements reported by Koltover *et al.*[8] an exact match of the electrochemical potentials of the different ionic species leads to PB solutions that agree with the major tendency of d_{DNA} vs c^* experimental curves, whereas complete disagreement remains if this condition is not imposed. These differences are also found on another structural property, namely, the profile distribution of mobile cationic lipids on charged membranes. The magnitude of this profile turned out to be lower than for the cases where the exact ion's chemical equilibrium was neglected.

II. MEAN-FIELD THEORY

We consider the system's unit cell shown in Fig. 1 formed by two flat lipid bilayers separated by the mean distance d_w. Each membrane has a thickness d_m, and it is formed by a mixture of cationic lipid dioleoyl trimethylammonium propane (TAP) at molar fraction ϕ_{TAP} and neutral colipid dioleoyl phosphatidylcholin. The total surface density σ_T of lipids on the membrane is given by the surface density σ of positive ones, with the average area available to each of the lipid's head group being $a=70$ Å^2, roughly the same for the neutral component.[8] The water phase in-between the lipid bilayers has a dielectric constant $\epsilon=78$ and contains a univalent electrolyte at concentration c^*. In the aqueous region there are two DNA macromolecules whose center to center distance d_{DNA} defines the lateral size of the cell of depth h.

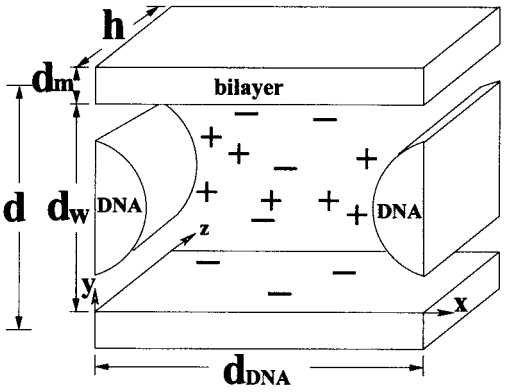

FIG. 1. Unit cell of DNA and lipid self-assembly. Two parallel slabs of cationic lipid bilayers enclosing two halves of DNA molecules and NaCl electrolyte.

At the mean-field level the free energy of the system's formation is, according to the theory of Harries *et al.*,[11,15]

$$F_c=(f_{\mathrm{field}}+f_{\mathrm{ion}}+f_{\mathrm{lipid}})h, \tag{1}$$

where

$$f_{\mathrm{field}}=\frac{\varepsilon}{8\pi}\int_0^{d_{\mathrm{DNA}}}dx\int_0^{d_w}dy(\nabla\psi)^2, \tag{2}$$

is Maxwell's electric-field stress contribution. The second term in F_c is the entropy of the mixing of pointlike ions and water molecules,

$$f_{\mathrm{ion}}=k_{\mathrm{B}}T\int_0^{d_{\mathrm{DNA}}}dx\int_0^{d_w}dy\left(c^+\ln\left[\frac{c^+}{c^*}\right]+c^-\ln\left[\frac{c^-}{c^*}\right]-(c^++c^--2c^*)\right). \tag{3}$$

In the approach of Harries *et al.*, the lipid size and the mobility on the lipid bilayers are taken into account through a corresponding entropy term,

$$f_{\mathrm{lipid}}=2k_{\mathrm{B}}T\int_0^{d_{\mathrm{DNA}}}dx\left\{\sigma\ln\left[\frac{\sigma}{\sigma_T}\right]+(\sigma_T-\sigma)\ln\left[\frac{\sigma_T-\sigma}{\sigma_T}\right]\right\}, \tag{4}$$

with k_{B} being Boltzmann's constant and T being the temperature. Extremization of the free energy, Eq. (1), yields following Boltzmann's factors for the distribution of ions:

$$c^{\pm}=c^*e^{\mp ze\psi/k_{\mathrm{B}}T}, \tag{5}$$

which satisfies the following PB equation:

$$\nabla^2\psi=-\frac{4\pi}{\varepsilon}[+zec^+-zec^-]. \tag{6}$$

The potential ψ fulfills the following boundary conditions:

$$\nabla\psi\cdot\hat{\mathbf{n}}=\begin{cases}4\lambda/\varepsilon r_D, & \text{on DNA}\\ 4\pi\sigma(x)/\varepsilon, & \text{on membrane},\end{cases} \tag{7}$$

with $\hat{\mathbf{n}}$ being the unit normal to the dielectric boundaries and pointing into the aqueous phase. $r_D=10$ Å is the radius of the

DNA, which has bare linear charge density $\lambda=-e/1.7$ Å, and e is the elementary charge. Further minimization of Eq. (1) with $\sigma(x)$ subject to the local charge constraint on bilayers, second part of Eq. (7), yields[11]

$$\sigma(x)=\frac{e^{-(\psi+\lambda_L)}}{a[(1-\phi_{\mathrm{TAP}})/\phi_{\mathrm{TAP}}+e^{-(\psi+\lambda_L)}]}. \tag{8}$$

In this equation the value of Lagrange's (L) multiplier λ_L is fixed by the requirement that, at equilibrium, for a given liposomal membrane charge density $e\phi_{\mathrm{TAP}}/a$, the local density $\sigma(x)$ on the corresponding membrane in the CL-DNA system must satisfy the following electroneutrality condition:

$$e\int_0^{d_{\mathrm{DNA}}} dx\sigma(x)-\frac{e\phi_{\mathrm{TAP}}}{a}=0. \tag{9}$$

III. RESULTS AND DISCUSSION

A. Compressibility modulus of DNA

The recent x-ray synchrotron experiments by Salditt *et al.*[5,6] revealed that DNA strands in the CL-DNA complex experience an effective repulsive force whose magnitude is given in Fig. 2 by the compressibility modulus B as a function of interhelical separation d_{DNA}. Such data were taken for eight different isoelectric systems where the cationic lipids are exactly neutralized by the anionic phosphate groups of the DNA. This amounts to a constant (DOTAP)/DNA weight ratio of 2.2 in all cases. Meanwhile the total lipid composition for each system was kept constant. Thus, the weight ratios of both types of lipids forming the lipid bilayers were varied eight times leading to a sequence of cationic lipid molar fractions whose values $\phi_{\mathrm{TAP}}=1$, 0.7407, 0.598, 0.5, 0.4, 0.3401, 0.3, and 0.25, and correspond to different measured equilibrium interhelical separations $d_{\mathrm{DNA}}=27.6$, 28.7, 38.1, 38.9, 47.9, 52.4, 53.0, and 54.7 Å associated to each of those isoelectric complexes, respectively. Wagner *et al.*[16] demonstrated that the formation of the lamellar CL-DNA phase is driven by counterion release both from the cationic lipids and from the DNA. Yet, it is maximal at the isoelectric point, where the estimated concentration of counterions was about 1 mM. Moreover, their study emphasized the importance of the very large entropic free-energy gain by released counterions that leads to the effective entropic force driving the association between the DNA and the lipids. In our calculations described below this force of entropic origin is embodied and taken implicitly into account in the electrostatic free energy, Eq. (1). Hence, the equilibrium spacing between DNA chains results from three forces: the attractive van der Waals force that tends to decrease DNA interhelical distance and the two repulsive forces that increase such separation, namely, the hydration and the electrostatic repulsion. The van der Waals interaction between two DNA molecules (modeled as two dielectric cylinders with a dielectric constant of 4) with a distance d_{DNA} apart is given through the following compressibility modulus:

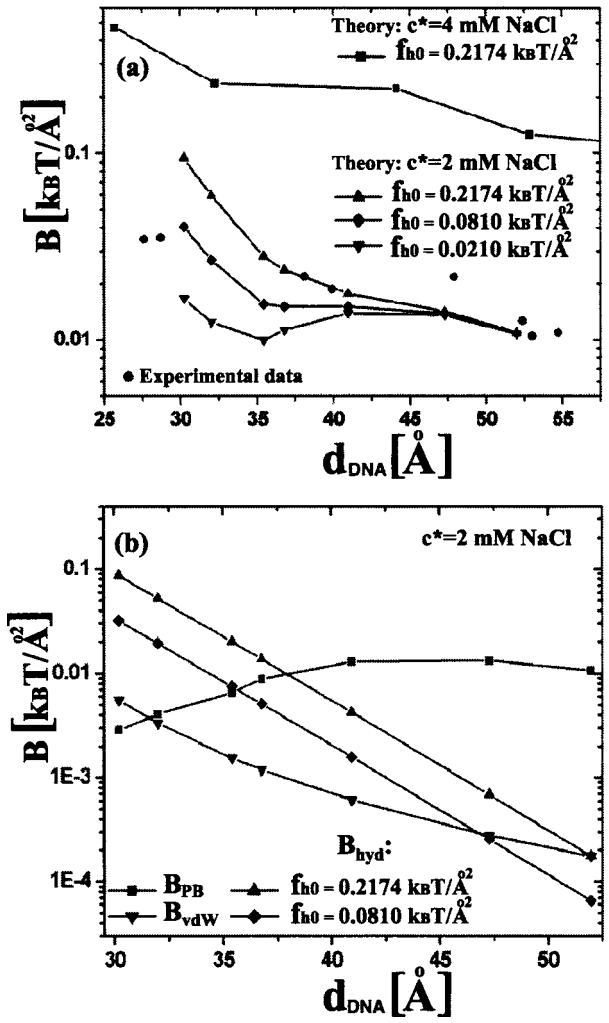

FIG. 2. Comparison of experimental data on DNA's compressibility modulus B with theory results, as a function of interhelical spacing d_{DNA} (a). All components of B are given in (b) at salt concentration $c^*=0.2$ mM for the eight isoelectric complexes considered in (a). The solid lines are guides to the eye.

$$B_{vdW}(d_{\mathrm{DNA}})=\frac{5A\sqrt{r_D}}{32}\frac{d_{\mathrm{DNA}}}{(d_{\mathrm{DNA}}-2r_D)^{7/2}}, \tag{10}$$

with the Hamaker constant $A=5.2\times10^{-21}$ J.[5] While the hydration contribution to the compressibility was derived in Ref. 5 from the empirically parametrized expression of the hydration force (having a spatial range of 30 Å) for bulk hexagonal DNA phases,

$$B_{\mathrm{hyd}}=d_{\mathrm{DNA}}\frac{f_{h0}}{\lambda_H}e^{-(d_{\mathrm{DNA}}-2r_D)/\lambda_H}, \tag{11}$$

where the observed exponential decay of this repulsive interaction, the force coefficient $f_{h0}=0.2174k_{\mathrm{B}}T/\text{Å}^2$, and decay length $\lambda_H=3.1-3.5$ Å were measured with osmotic stress techniques by Podgornik *et al.*[17] For the condensed DNA inside the complex, it was found in Ref. 5 that in highly screened isoelectric complexes by NaCl electrolyte in solution, hydration interaction prevails over the electrostatic one producing DNA separations of the order of 30 Å, similar to what it is observed in bulk 3D DNA hexatic phases,[17] in spite of confinement and geometrical restrictions prevailing inside

TABLE I. Experimental values of isoelectric CL-DNA system cell size at $c^*=0.0$ mM of NaCl.

ϕ_{TAP}	d(Å)[a]	d_m(Å)[a]	d_w(Å)[b]
0.3	71.33	42.0	29.33
0.4	68.0	39.97[c]	28.03
0.5	66.38[c]	38.2	28.18
0.6	64.89	37.39[c]	27.5
0.7	63.42	36.67[c]	26.75
0.8	61.91[c]	35.9[c]	26.01
1.0	59.12	34.5	24.62

[a]Taken from Ref. 8.
[b]From $d_m=d-d_w$.
[c]Extrapolated.

the complex. Therefore, we use in this paper the above phenomenological parametrization of B_{hyd} with f_{h0} and λ_H as fitting force parameters. Finally, the long-range contribution to the compressibility arising from electrostatic interactions (with its main contribution resulting from the ion's entropic force) becomes important at separations larger than 30 Å. We calculated it numerically from the free energy F_c of Eq. (1) per unit *area* of the complex using the following thermodynamic relationship:

$$B_{\mathrm{PB}} = d_{\mathrm{DNA}}^2 \left. \frac{\partial^2 (F_c(l)/\mathrm{area})}{(\partial l)^2} \right|_{l=d_{\mathrm{DNA}}}. \tag{12}$$

When using Eq. (12), we first determined the complex's free energy F_c, Eq. (1), as a function of several DNA spacings l at constant ϕ_{TAP} and electrolyte concentration c^*. The minimum of F_c sets in the thermally equilibrated DNA separation $l=d_{\mathrm{DNA}}$. Thereafter, B_{PB} is evaluated from Eq. (12) at this constant d_{DNA}, which comes about from the given ϕ_{TAP} corresponding to one isoelectric complex. In this manner, the mean-field prediction of the compressibility was obtained for each of the eight different molar fractions corresponding to the various isoelectric systems quoted above. We considered the system's unit-cell sizes given in Table I. Thus, the total compressibility modulus is $B=B_{\mathrm{PB}}+B_{\mathrm{hyd}}+B_{\mathrm{vdW}}$, which we plotted and compared with the experimental data in Fig. 2(a). The comparison is made using three constant force parameters $f_{h0}=(0.2174, 0.081, \text{and } 0.02108)k_{\mathrm{B}}T/\text{Å}^2$, and a fixed space decay length $\lambda_H=3.23$ Å in all cases. B_{PB} was calculated using salt concentrations $c^*=2$ and 4 mM (with $f_{h0}=0.2174k_{\mathrm{B}}T/\text{Å}^2$ and $\lambda_H=3.23$ Å for the latter concentration). It can be observed in Fig. 2(a) that the prediction for B agrees with the experiment for interchain separations $d_{\mathrm{DNA}} \geqslant 33$ Å using a fit of hydration B_{hyd} with $f_{h0}=0.2174k_{\mathrm{B}}T/\text{Å}^2$, $\lambda_H=3.23$ Å, and $c^*=2$ mM. However, it deviates substantially from the experimental value for $d_{\mathrm{DNA}}<33$ Å. In Fig. 2(b) all components of B for $c^*=2$ mM are shown as a function of d_{DNA}. It can be noted that the case of the best fit to the experimental data has a hydration contribution B_{hyd} that overwhelms the electrostatic part B_{PB} in the range $d_{\mathrm{DNA}}<33$ Å. Yet, with a selection of different values of f_{h0}, λ_H does not even improve the prediction of B. The availability of more complete sets of experimental measurements of the hydration force in this self-assembled system would be desirable, as has been done already in a very accurate and exhaustive form for biomembrane bilayers at physiological salt concentrations in solution.[18,19]

B. Adsorption isotherms of DNA and lipids

In our calculations outlined above, we assumed that both the chemical potentials of negative μ^- and positive μ^+ ions are equal, which imply that their bulk concentration are the same, $c^*\Lambda^3=\exp[\beta\mu^+]=\exp[\beta\mu^-]$, with $\Lambda=\Lambda^+=\Lambda^-$ the thermal wavelength. In what follows we relax this approximation and take into account their real chemical potentials, which are in fact different, $\mu^+=\mu_\pm^{\mathrm{bulk}}+\chi$ and $\mu^-=\mu_\pm^{\mathrm{bulk}}-\chi$ where at chemical equilibrium $\exp[\beta\mu_\pm^{\mathrm{bulk}}]=c^*\Lambda^3\gamma_\pm$, with $\gamma_\pm$ being the mean activity coefficient. Then, the profile counterion distributions are $c^\nu=e^{\beta\mu_\nu}/\Lambda^3\gamma^\nu$ with $\nu=\pm$ and $\beta=1/k_{\mathrm{B}}T$. γ^+ and γ^- are the activity coefficients of each ionic species. The overall electroneutrality condition of the system determines χ according to

$$\int_0^{d_{\mathrm{DNA}}} dx \int_0^{d_w} dy[+zec^+(x,y) - zec^-(x,y)] + 2e\int_0^{d_{\mathrm{DNA}}} dx\sigma(x) = |\lambda|. \tag{13}$$

Koltover *et al.*[8] reported a series of measurements performed on isoelectric CL-DNA complexes. They determined the dependence of DNA spacing d_{DNA} with added univalent salt NaCl at concentration c^* for different charged membranes as given by their cationic molar fraction ϕ_{TAP}. Koltover *et al.* found, at low $\phi_{\mathrm{TAP}}<0.6$, a nonmonotonous variation of d_{DNA} for increasing ionic strength c^*. They observed that DNA separation d_{DNA} increases slowly starting from small c^*, with a sudden drop in the magnitude of the DNA interhelical separations at high salt concentration (which value depends on ϕ_{TAP}). Such a sharp change of the d_{DNA} adsorption isotherm is ascribed to the CL-DNA system instability that occurs because both DNA molecules and cationic lipids are released from the system due to the high salt screening of the counterion release mechanism.[8] At higher $\phi_{\mathrm{TAP}} \geqslant 0.6$ of the membrane charge, the effect of c^* on d_{DNA} manifests through an observed swelling of the system's stack of bilayers, with a simultaneous monotonous increase of DNA average separations for increasing c^*. At these high salt contents direct DNA-DNA electrostatic interaction is screened and hydration repulsion was found to prevail between DNA strands, which contributes to the set an equilibrium d_{DNA} distance of separation of a range of 30 Å.[8] In Fig. 3 we show our calculated complexation isotherms of d_{DNA} vs c^* and their comparison with the experimental data of Koltover *et al.* (black-filled circles joined by line) for $\phi_{\mathrm{TAP}} \geqslant 0.6$. In the approximate case of equal ion's chemical potentials $\mu^+=\mu^-=\mu_\pm^{\mathrm{bulk}}$ ($\chi=0$, black-filled squares joined by line), and the case with an exact match of real chemical potentials of ions inside the complex $\mu^\pm$ with that for ions in bulk solution $\mu_\pm^{\mathrm{bulk}}$, ($\mu^\pm=\mu_\pm^{\mathrm{bulk}}\pm\chi$, black-filled triangle up symbols, $\chi\neq 0$). In order to determine correctly in each case $\mu^\pm$ we use Ref. 20, that contains measured mean activity coefficients $\gamma_\pm$ as a function of concentrations c^* of the electrolyte NaCl. The

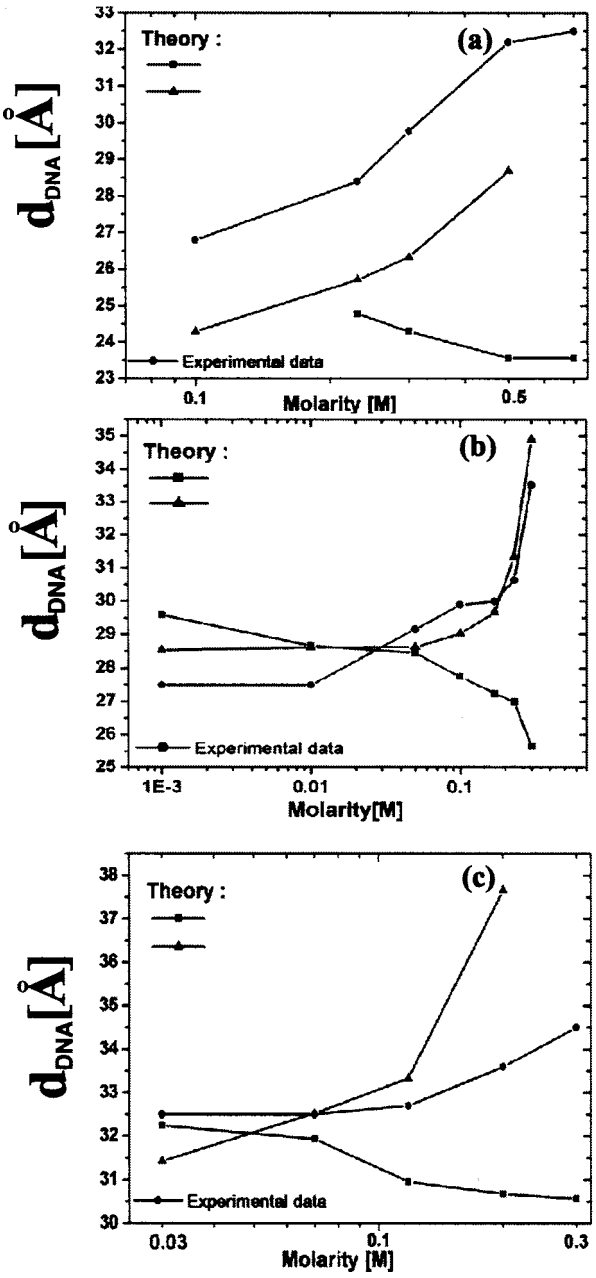

FIG. 3. Complexation isotherms of DNA and lipids, given as curves of d_{DNA} vs concentration c^* of salt NaCl for molar fractions of charged lipids on membrane $\phi_{\mathrm{TAP}}=0.9$ (a), 0.7 (b), and 0.6 (c), respectively. In all plots, theory predictions are depicted with $\chi\neq 0$ exact match of ion's chemical potentials ($\mu^{\pm}=\mu_{\pm}^{\mathrm{bulk}}\pm\chi$, with □ symbols) and under the approximation $\mu^{+}=\mu^{-}$ ($\chi=0$, with △ symbols). The solid lines are guides to the eye.

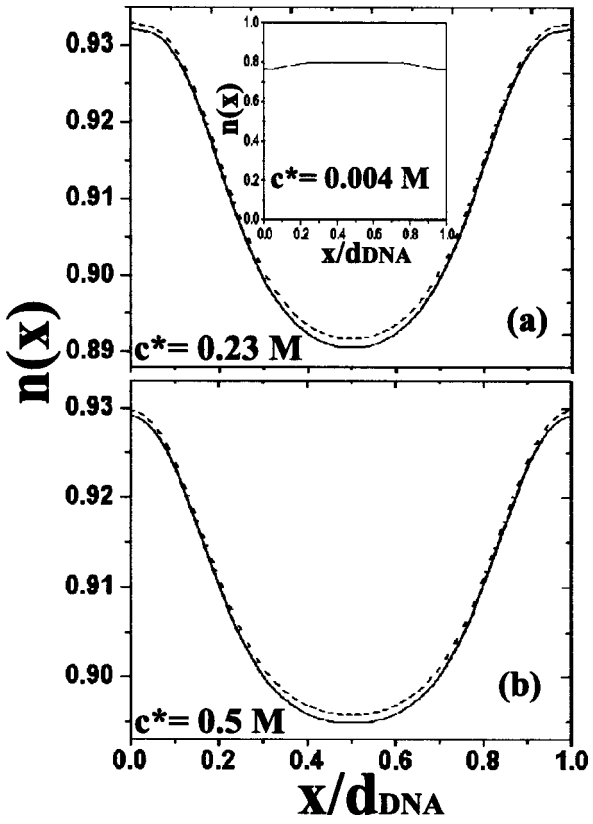

FIG. 4. Nondimensionalized density profile of positive lipids $n(x)$ vs DNA spacing d_{DNA}. The case of fixed cationic lipid molar fraction $\phi_{\mathrm{TAP}}=0.9$ on the bilayer and two salt concentrations $c^*=0.23M$ (a) and $0.5M$ (b). Theory calculations with $\mu^{+}=\mu^{-}$ as a condition for ion's chemical equilibrium ($\chi=0$, dash line) and $\chi\neq 0$ (continuous line). In (a) and (b) are shown the large segregation of lipids produced by inhomogeneous screening of ions on the DNA's and bilayer's electric fields due to the high salt concentration. Positive ions form a void in the spatial region $0<x/l_D<1.0$ around the DNA molecule, while negative ions deplete from this region accumulating more in the middle of the cell (see also Fig. 6). The inset in (a) at $\phi_{\mathrm{TAP}}=0.78$ shows that lipid segregation on the bilayer is almost negligible when the salt content in the solution is very small.

system's unit-cell sizes d and d_w used in the numerical calculations of F_c were taken from Table I. Additionally, useful values of d_{DNA} and d were read off from Fig. 6(d) of Ref. 8. We used a cell depth $h=1$ Å. The main features of the calculated d_{DNA} vs c^* curves is that they generally follow the trends of the corresponding experimental curves when the correct ion's chemical potentials ($\mu^{\pm}=\mu_{\pm}^{\mathrm{bulk}}\pm\chi$) are taken into account. However, the prediction disagrees with the experiment when the approximation $\mu^{+}=\mu^{-}$, that is, Eq. (5) is used. These results show that it is not realistic to assume as a chemical equilibrium condition equal chemical potentials, $\mu^{+}=\mu^{-}$, for the different kinds of ions that reside in the inner side of the complex, with those of ions in the exterior aqueous phase. Rather, the equilibrium value of $\mu^{\pm}=\mu_{\pm}^{\mathrm{bulk}}\pm\chi$ for each ion's species should be used. It should be noted that for the calculated curves in Fig. 3 we did not consider the hydration and the van der Waals contributions to the free energy F_c but only the long-range electrostatic part, that is, Eqs. (1)–(9) together with Eq. (13). We also performed numerical calculations of d_{DNA} curves as a function of c^* including the DNA-DNA phenomenological bulk hydration (hyd) interaction energy $F_{\mathrm{hyd}}=-f_{h0}\lambda_H[\exp[-(d_{\mathrm{DNA}}-2r_D)/\lambda_H]-1]$,[17] into F_c. Since F_{hyd} is c^*'s independent, the overall effect of F_{hyd} is to shift the magnitude of F_c, but does not change the location of its minimum localized at $l=d_{\mathrm{DNA}}$. Therefore, the inclusion of bulk hydration repulsion into F_c leads to the same results as in the case when it is neglected. Thus, the same curves of Fig. 3 are obtained. However, we believe that F_{hyd} depends on the confining geometry as presented in the CL-DNA complex. Yet, there remains its comprehensive experimental determination in order to be incorporated in a theoretical framework as discussed here. A similar study for the low charged membrane cases $\phi_{\mathrm{TAP}}<0.6$ can be made.

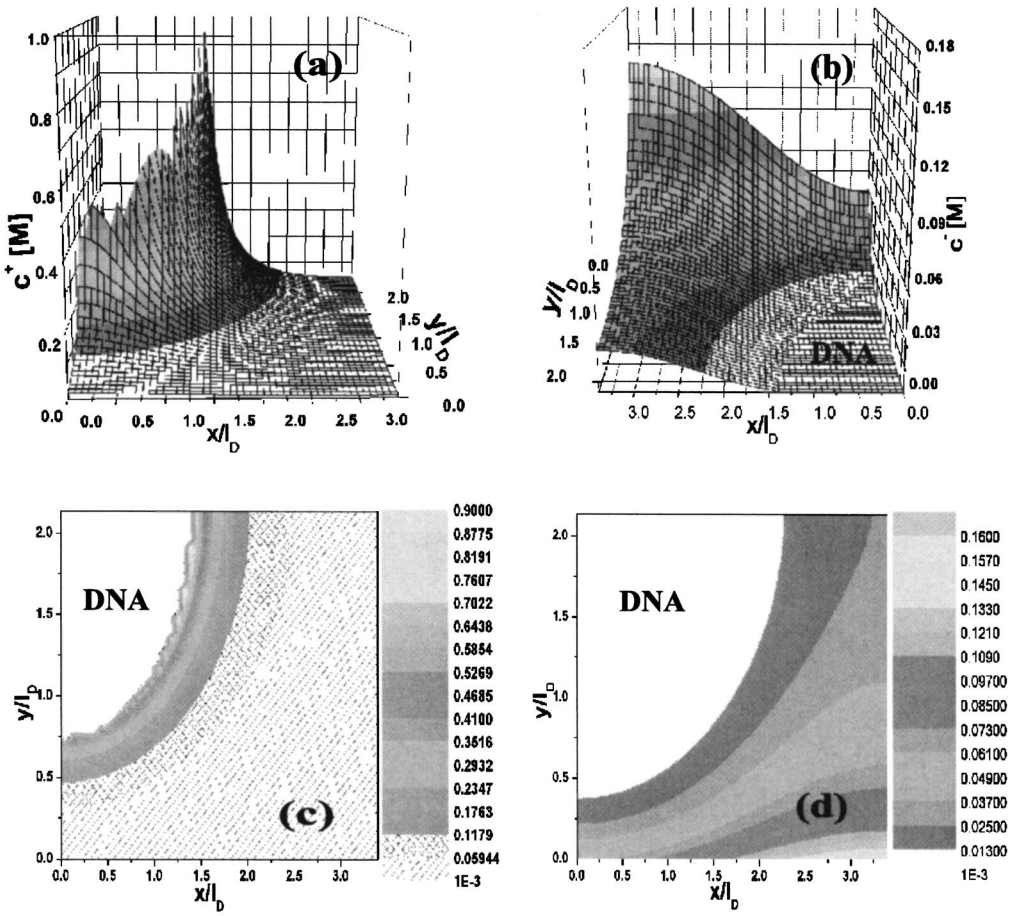

FIG. 5. Density functions of positive c^+ (a) and negative c^- (b) ions around the DNA molecule, and their contour plots (c) and (d), respectively. The molar fraction of charged lipids on the membrane is $\phi_{\mathrm{TAP}}=0.3$ with aqueous NaCl concentration $c^*=0.23M$. Note in (c) the compact double layer formed by positive ions around the DNA.

C. Profile distribution of cationic lipids

The exact match condition on the chemical potentials of the ions also shows qualitative effects on another relevant structural property: the charge modulation of positive lipids on membranes, $n(x) \coloneqq \sigma(x)a$. In Fig. 4 we give examples of nondimensionalized cationic lipid density profiles $n(x)$ at two electrolyte concentrations $c^*=0.23M$ and $0.5M$ for unit-cell sizes $d_{\mathrm{DNA}}=6.802l_D$, d_w (taken from Table I), and $h=1$ Å$[l_D=\sqrt{(\varepsilon k_{\mathrm{B}}T/4\pi c^* e^2)}]$. For their determination we do not include neither the hydration nor the van der Waals effects in F_c. This corresponds to an isoelectric CL-DNA system at $\phi_{\mathrm{TAP}}=0.9$ of cationic lipids (highly charged membrane). Note that $n(x)$ is symmetrical around the midplane between DNA molecules. The most important feature is the accumulation of the cationic lipids close to and on top of the DNA cylindrical surface centered at the end sides of the cell located at $x=0.0d_{\mathrm{DNA}}$ and $x=d_{\mathrm{DNA}}$ with a large depletion of lipids at the midplane. The segregation of lipids observed in Fig. 4 results from the high salt content. Thus, for instance, if we reduce its strength by three orders of magnitude to $c^*=0.004M$ and consider a less charged membrane case $\phi_{\mathrm{TAP}}=0.78$, then, the profile $n(x)$ displays very little segregation of lipids, as can be noted in the inset of Fig. 4(a).

When we made use of $\mu^+=\mu^-$ as the chemical equilibrium of ions and $c^*=0.23M$ salt concentration [Fig. 4(a), dash line], the profile $n(x)$ is larger than the profile of positive lipids at the higher ionic strength $c^*=0.5M$ [Fig. 4(b), dash line], and both profiles obtain their maximum magnitudes in the spatial regimes $0\leqslant x\leqslant 0.1d_{\mathrm{DNA}}$ and $0.9d_{\mathrm{DNA}}\leqslant x\leqslant d_{\mathrm{DNA}}$ close to the DNA molecules (recall $\phi_{\mathrm{TAP}}=0.9$). This phenomenon results from the more effective lipid's screening to the DNA electric field close to the membrane (for $c^*=0.23M$), where cationic lipids see an imperfectly charge-neutralized DNA molecule by the salt ions. Positive ions form a void in the region of closest approach of the DNA surface to the membrane, while negative ions deflect and get concentrated more in the middle of the cell (see Fig. 6 below). Therefore, at $c^*=0.23M$, the DNA electric field makes the cationic lipids to be crowded where the DNA field is higher, implying a better charge matching on the DNA and membrane. A more realistic determination of the trends of lipid membrane modulations turns out when we use $\mu^{\pm}=\mu_{\pm}^{\mathrm{bulk}}\pm\chi$ for the ion's chemical equilibrium (see curves in Fig. 4 with black continuous lines for $c^*=0.23M$ and $c^*=0.5M$). Small quantitative deviations are obtained with respect to the profiles derived with $\mu^+=\mu^-$ as a condition. This only indicates that both models are not equivalent, with the

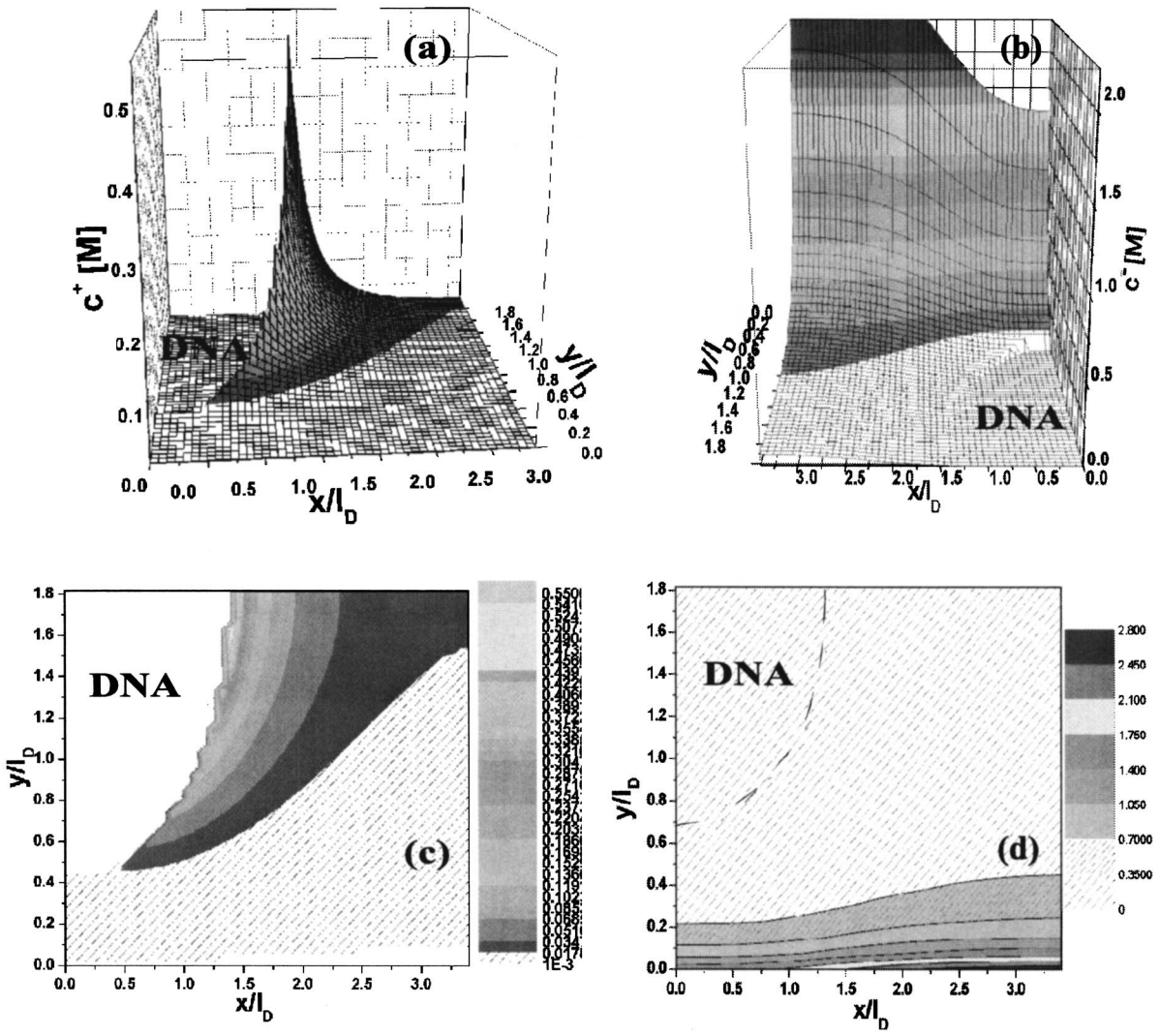

FIG. 6. Same as Fig. 5 for ion's distribution functions c^+ and c^- with $\phi_{\mathrm{TAP}}=0.9$ and $c^*=0.23M$. Inside (c) there is a region of vacuum, $0<x/l_D<0.5$, formed by positive ions on the surface of the DNA, while they are concentrated more in the space between DNA strands. (d) depicts the large accumulation of negative ions onto the lipid bilayer. They form a narrow cloud that shows the depletion of ions close to the DNA surface.

former ($\chi\neq 0$) being more accurate. We found, however, that the expression $\mu^{\pm}=\mu_{\pm}^{\mathrm{bulk}}\pm\chi$ leads to similar predictions as with $\chi=0$.

D. Local-density functions of ions

The ion's distribution functions $c^{\pm}(x,y)$ are shown as perspective plots in Figs. 5(a) and 5(b), together with their complementary contour plots in Figs. 5(c) and 5(d), respectively. These profile distributions were obtained for a system with unit-cell sizes $d_{\mathrm{DNA}}=6.802l_D$, d_w from Table I, and with $h=1$ Å and $c^*=0.23M$ NaCl salt, and using $\mu^{\pm}=\mu_{\pm}^{\mathrm{bulk}}\pm\chi$ for the case of an almost neutral membrane $\phi_{\mathrm{TAP}}=0.3$. Figure 5 refers only to one quarter cell of Fig. 1. Note in Fig. 5(a) that positive ions c^+ form a rather compact double layer around the DNA surface, and they are pushed away from the cationic lipid bilayer located at $y/l_D=0$ [front face of the cubic cell of Fig. 5(a)], meanwhile they are more concentrated at the side $y/l_D=2.3$ ($=d_w/2l_D$ distance away from front face of the cell) where c^+ shows a maximum. The contour plot of c^+ in Fig. 5(c) depicts the compactness of the positive ion's double layer about the DNA with a void of positive ions in any other region in the cell. If the molar fraction is increased up to $\phi_{\mathrm{TAP}}=0.9$, the maximum of c^+ appearing at $y=2.3l_D$ diminishes with the positive ions spreading out mainly inbetween DNA molecules, while the profile strength c^+ at $(x/l_D,y/l_D)\approx(0,1.5)$, that is, towards the membrane side, gets lower showing a vacuum of ions in the region $0<x/l_D<1.0$ [see Fig. 6(a)]. The distribution function $c^-(x,y)$ takes on quite a different appearance as shown in Fig. 5(b). Negative ions have a more widespread distribution in all of the aqueous phase available in the cell and tend to occupy all the space in an inhomogeneous manner, showing their highest condensation close to the membrane for $\phi_{\mathrm{TAP}}=0.3$ [Figs. 5(b) and 5(d)]. In this case c^- is high near the lipid membrane located at $y/l_D=0.0$ where there is better electrostatic matching, but with a depletion of ions about $x/l_D=0.0$ due to electrostatic repulsion with the smeared negative charge on the DNA. In the case of $\phi_{\mathrm{TAP}}=0.9$ and $c^*=0.23M$, both the profile distribution $c^-(x,y)$ of Fig. 6(b) and its contour plot in Fig. 6(d) show that negative ions are tightly condensed onto the liposomal membrane with a depletion of ions close to the DNA surface while they accumulate more at the middle of

the cell. Thus, they present a strong inhomogeneous screening to the electric field emanating from the cationic lipids, which in turn get more concentrated near the DNA molecule. This fact was already noted also in Sec. III C, where a large spatial segregation of lipids in the unit cell was observed [see Figs. 4(a) and 4(b)], which is more emphasized than in the case of small salt content $c^*=0.004M$ at the same $\phi_{\mathrm{TAP}}=0.9$. Its corresponding function $n(x)$ of charge modulation of lipids is almost flat, reflecting its constant spatial variation as depicted in the inset of Fig. 4(a).

IV. CONCLUSION

In this paper we have made a comparison between experiments and mean-field PB theory results, of the DNA's compressibility modulus of lamellar cationic lipid-DNA systems at the isoelectric state. Our numerical results emphasized the importance of hydration repulsion on the compressibility modulus of DNA molecules. Hydration interaction becomes the main effect on this thermodynamic property at short-range interhelical separations, whereas at larger separations the long-range electrostatic contribution dominates. Since the DNA interhelical spacing dependence of hydration repulsion has not been measured systematically at different system's conditions of membrane charge, added salt, DNA/lipid charge ratio, etc., we used the experimentally parametrized form of this interaction, which is valid only for 3D bulk DNA phases in solution. A fit of the hydration force contribution into the theoretical compressibility modulus of the CL-DNA system leads to partial agreement with the experimental data at large DNA separations ($d_{\mathrm{DNA}}>33$ Å). However, at shorter separations ($d_{\mathrm{DNA}}<33$ Å) the predicted B deviates substantially from observations.

We also showed the importance of taking correctly into account within the PB theory the exact match of the electrochemical potentials of the different ionic species. The resulting chemical equilibrium condition leads to qualitative agreement between the theory and the observed trends of complexation isotherms of DNA plus lipid's adsorption in these self-assemblies.

ACKNOWLEDGMENTS

We would like to thank Professor M. Medina-Noyola for his kind revision of this paper. This work was supported by CONACyT Grant No. 36557-E, Mexico.

[1] L. Huang, M. Huang, and E. Wagner, *Nonviral Vectors for Gene Therapy* (Academic, San Diego, 1999).
[2] J. A. Wolff, *Gene Therapeuthics: Methods and Applications of Direct Gene Transfer* (Birkhauser, Boston, 1994).
[3] C. R. Safinya, Curr. Opin. Struct. Biol. **11**, 440 (2001).
[4] P. L. Felgner, Sci. Am. **276**, 102 (1997).
[5] T. Salditt, I. Koltover, J. O. Rädler, and C. R. Safinya, Phys. Rev. E **58**, 889 (1998).
[6] T. Salditt, I. Koltover, J. O. Rädler, and C. R. Safinya, Phys. Rev. Lett. **79**, 2582 (1997).
[7] J. O. Rädler, I. Koltover, T. Salditt, and C. R. Safinya, Science **275**, 810 (1997).
[8] I. Koltover, T. Salditt, and C. R. Safinya, Biophys. J. **77**, 915 (1999).
[9] A. J. Lin, N. L. Slack, A. Ahmad, C. X. George, C. E. Samuel, and C. R. Safinya, Biophys. J. **84**, 3307 (2003).
[10] R. Bruinsma and J. Mashl, Europhys. Lett. **41**, 165 (1998).
[11] D. Harries, S. May, W. M. Gelbart, and A. Ben-Shaul, Biophys. J. **75**, 159 (1998).
[12] O. González-Amezcua and M. Hernández-Contreras, J. Chem. Phys. **121**, 10742 (2004).
[13] S. May, D. Harries, and A. Ben-Shaul, Biophys. J. **78**, 1681 (2000).
[14] D. Harries, S. May, and A. Ben-Shaul, J. Phys. Chem. B **107**, 3624 (2003).
[15] R. Lipowsky and E. Sackmann, *Structure and Dynamics of Membranes* (Elsevier, Amsterdam, 1995).
[16] K. Wagner, D. Harries, S. May, V. Kahl, J. O. Rädler, and A. Ben-Shaul, Langmuir **16**, 303 (2000).
[17] R. Podgornik, D. C. Rau, and V. A. Parsegian, Biophys. J. **66**, 962 (1994).
[18] A. C. Cowley, N. L. Fuller, R. P. Rand, and V. A. Parsegian, Biochemistry **17**, 3163 (1978).
[19] A. Parsegian, N. Fuller, and R. P. Rand, Proc. Natl. Acad. Sci. U.S.A. **76**, 2750 (1979).
[20] V. M. M. Lobo and J. L. Quaresma, *Handbook of Electrolyte Solutions* (Elsevier, Amsterdam, 1989).